A&A 443, 735–746 (2005)
DOI: 10.1051/0004-6361:20053511

Astronomy & Astrophysics

A library of high resolution synthetic stellar spectra from 300 nm to 1.8 μm with solar and α-enhanced composition⋆,⋆⋆

P. Coelho[1,2], B. Barbuy[1], J. Meléndez[3], R. P. Schiavon[4], and B. V. Castilho[5]

[1] Universidade de São Paulo, Rua do Matão 1226, São Paulo 05508-900, Brazil
e-mail: pcoelho@usp.br;barbuy@astro.iag.usp.br
[2] Max-Planck-Institut für Astrophysik, Karl-Schwarzschild-Strasse 1, 85741 Garching, Germany
e-mail: pcoelho@mpa-garching.mpg.de
[3] Department of Astronomy, Caltech, 1200 E. California Blvd, Pasadena, CA 91125, USA
e-mail: jorge@astro.caltech.edu
[4] Department of Astronomy, University of Virginia, PO Box 3818, Charlottesville, VA 22903-0818, USA
e-mail: ripisc@virginia.edu
[5] Laboratório Nacional de Astrofísica / MCT, CP 21, 37500-000 Itajubá, Brazil
e-mail: bruno@lna.br

Received 25 May 2005 / Accepted 21 July 2005

ABSTRACT

Libraries of stellar spectra are fundamental tools for the study of stellar populations, and both empirical and synthetic libraries have been used for this purpose. In this paper, a new library of high resolution synthetic spectra is presented, ranging from the near-ultraviolet (300 nm) to the near-infrared (1.8 μm). The library spans all the stellar types that are relevant to the integrated light of old and intermediate-age stellar populations in the involved spectral region (spectral types F through M and all luminosity classes). The grid was computed for metallicities ranging from [Fe/H] = –2.5 to +0.5, including both solar and α-enhanced ([α/Fe] = 0.4) chemical compositions. The synthetic spectra are a good match to observations of stars throughout the stellar parameter space encompassed by the library and over the whole spectral region covered by the computations.

Key words. stars: atmospheres

1. Introduction

Libraries of stellar spectra are one of the main ingredients of stellar population synthesis models (e.g. Bruzual & Charlot 1993, 2003; Cerviño & Mas-Hesse 1994; Fioc & Rocca-Volmerange 1997; Leitherer et al. 1999; Vazdekis 1999; Buzzoni 2002; Schulz et al. 2002; Jimenez et al. 2004; Gonzalez Delgado et al. 2005; Maraston 2005; Schiavon 2005) and both empirical and theoretical libraries have improved dramatically in recent years. The first empirical libraries (e.g. Gunn & Stryker 1983; Jacoby et al. 1984) used in stellar population synthesis work were restricted to a relatively small number of stars with uncertain atmospheric parameters. The quality of empirical libraries has been refined through the years (e.g. Pickles 1998; Jones 1999) and recently, a major improvement has been achieved by Le Borgne et al. (2003; STELIB) and Valdes et al. (2004; Indo-US), who together provide high S/N, medium resolution (down to *FWHM* ∼ 1 Å) and a good coverage of the color-magnitude diagram.

Amongst the synthetic libraries, perhaps the most widely used is the flux distribution predicted from the Kurucz (1993) model atmospheres. Lejeune et al. (1997, 1998) and Westera et al. (2002) extended this library to include spectra of M stars computed from model atmospheres from Fluks et al. (1994), Bessell et al. (1989), Bessell (1991), and Allard & Hauschildt (1995). Moreover, they calibrated the flux distribution of the synthetic spectra in order to match the colors of observed stars (BaSeL library). However, the spectral resolution of the BaSeL library is limited to the sampling of the model atmosphere grid (∼20 Å), which is lower by far than the modern observed spectra of both individual stars and integrated stellar populations. More recently, resolution thus ceased to be a limitation, with the publication of high resolution spectral libraries by Chavez et al. (1997), Murphy & Meiksin (2004), Martins et al. (2005), and Rodrigues-Merino et al. (2005). However, these theoretical libraries still have a more limited wavelength coverage than that of the previous low-resolution synthetic libraries.

The choice of using either an empirical or a synthetic library in stellar population models is a subject of debate in the literature. One disadvantage of synthetic libraries is that they

⋆ The library of spectra is available in FITS format upon request to the authors, or in ASC format at the CDS via anonymous ftp to cdsarc.u-strasbg.fr (130.79.128.5) or via http://cdsweb.u-strasbg.fr/cgi-bin/qcat?J/A+A/443/735
⋆⋆ Appendix A is only available in electronic form at http://www.edpsciences.org

rely on model atmospheres, which are subject to systematic uncertainties. Besides, computing a reliable high-resolution synthetic spectral library for a wide range of stellar parameters and in a large spectral region is a very challenging task, because it requires building an extensive and reliable list of atomic and molecular line opacities which are needed for an accurate reproduction of high-resolution spectra of real stars. On the other hand, synthetic spectral libraries overcome limitations of empirical libraries, the most important being their inability to extrapolate to abundance patterns that differ from those of the library stars, which are from the solar neighbourhood or, in some cases, those of the Magellanic Clouds. Therefore, models based on empirical libraries cannot reproduce the integrated spectra of systems that have undergone star formation histories that are different from those of local systems.

The first compelling evidence that models based on empirical libraries have difficulty reproducing the integrated light of extra-galactic populations was presented by Worthey et al. (1992). These authors have shown that single stellar population synthesis models for the Lick/IDS indices (Burstein et al. 1984; Worthey et al. 1994; Trager et al. 1998) cannot reproduce the indices measured in giant elliptical galaxies, thus indicating that these systems are overabundant in α-elements relative to the Sun. This happens because, by construction, the abundance pattern of models based on empirical libraries is dictated by that of the library stars, which mirrors the abundance pattern of the solar neighborhood (but see discussion in Schiavon 2005). Therefore, such models are bound to follow the relation between [Fe/H] and [α/Fe] that is characteristic of the solar neighborhood where [α/Fe] is above solar at low metallicities and around solar in the high-metallicity regime (e.g. McWilliam 1997). As a result, the models cannot match the integrated light of metal-rich, α-enhanced systems, such as giant ellipticals.

This deficiency could, in principle, be partially cured empirically, by including spectra of bulge stars in the spectral libraries. The population of the bulge of the Galaxy has an α-enhanced abundance pattern even at high [Fe/H] (e.g. McWilliam & Rich 1994, 2004; Zoccali et al. 2004). However, their inclusion in sufficient numbers is hampered by their faintness and severe reddening, so that very few (or none) of these stars are included in empirical libraries.

For the case of the Lick/IDS indices, models that account for variable α-enhancement have been developed (e.g. Trager et al. 2000; Thomas et al. 2003a; Proctor et al. 2004; Tantalo et al. 2004; Mendes de Oliveira et al. 2005; Schiavon 2005). Even though the Lick/IDS indices have already proven their critical importance for the understanding of the stellar populations, it is crucial to develop models that can explore the huge amount of information contained in the whole spectrum, since methods fitting the entire spectrum are now feasible (Heavens et al. 2004; Panter et al. 2004).

Currently, the only way to produce models with abundance patterns that differ from those of the stars in the solar neighbourhood is through the adoption of synthetic stellar spectra. Although grids of high-resolution synthetic spectra have recently been computed, a wide grid with an α-enhanced mixture is still lacking. To our knowledge, so far two grids of synthetic spectra with α-enhanced mixtures have been available: Barbuy et al. (2003) published a grid in the wavelength range 4600−5600 Å aiming at the study of the effect of α-enhancement on the Lick/IDS indices Mg2, Fe5270, and Fe5335; and Zwitter et al. (2004) published a grid covering 7653−8747 Å, which is meant to be used with the spectroscopic surveys by RAVE and GAIA (Steinmetz 2003; Katz 2004).

In this work we present for the first time a grid of synthetic spectra covering solar and α-enhanced mixtures in a wide baseline. The grid is aimed at applications in stellar population synthesis, specifically to the study of old and intermediate-aged stellar populations. Thus, the grid covers the effective temperatures and surface gravities suitable for these systems.

We would like to emphasize, however, that applications of this grid are not limited to stellar population studies. The spectral library should also be a very useful tool for atmospheric parameter determination work, in particular as input in automatic procedures of deriving atmospheric parameters of a large number of observed stars (e.g. Cayrel et al. 1991a; Franchini et al. 2004; Willemsen et al. 2005; Girard & Soubiran 2005; Valenti & Fischer 2005).

This paper is organized as follows. In Sect. 2 we briefly describe the computation of the synthetic spectra and the production of the atomic and molecular line lists. Section 3 presents the library, and aspects of the relative contribution of the chemical species are investigated. A summary is given in Sect. 4.

2. Calculations

The spectra were computed using the code *PFANT*. The first version of this code named *FANTOM* was developed by Spite (1967) for the calculation of atomic lines. Barbuy (1982) included the calculation of molecular lines, implementing the dissociative equilibrium by Tsuji (1973) and molecular line computations as described in Cayrel et al. (1991b). It has been further improved for calculations of large wavelength coverage and inclusion of hydrogen lines as described in Barbuy et al. (2003). Ten hydrogen lines from H_{10} to H_α are considered through a revised version of the code presented in Praderie (1967). Higher order Balmer lines and Paschen and Brackett series are not yet considered in the present version of the code. Given a stellar model atmosphere and lists of atomic and molecular lines, the code computes a synthetic spectrum assuming local thermodynamic equilibrium.

The model atmospheres adopted were those presented by Castelli & Kurucz (2003), which account for α-enhanced compositions. The solar abundances adopted are those from Grevesse & Sauval (1998), which are consistent with the abundances used in the model atmospheres. These models differ from the previous ATLAS9 grid (Kurucz 1993), mainly because they include new opacity distribution functions and new molecular opacities, and do not include overshooting.

These models have mixing length parameter (ratio between the characteristic length and the scale height of the local pressure) of 2.0. A lower value ($l/H_P = 0.5$) was suggested by Fuhrmann et al. (1993) and Van 't Veer-Menneret & Mégessier (1996) as being more suitable for reproducing the profile of Balmer lines (as was adopted in the models in

Barbuy et al. 2003). But it is important to note that the Balmer lines are also not reproduced well because their cores are affected by the chromosphere and by departures from local thermodynamic equilibrium.

2.1. Atomic line opacities

Accurate line opacities are at the very heart of a successful synthetic spectrum computation. The line list employed here is an updated version of the one presented in Barbuy et al. (2003), where oscillator strengths (log gfs) and damping constants were revised.

The line list was extended up to 1.8 μm with the inclusion of the data from Meléndez & Barbuy (1999). The most recent oscillator strengths listed in the latest electronic version of the NIST database (Reader et al. 2002) were adopted. These values account for 10 to 50% of the lines in the near-UV and visible spectral regions, respectively. The log gf values of 139 Fe II lines were updated according to the normalisation given in Meléndez & Barbuy (2002). Line-by-line fits to the solar spectrum were done in specific spectral regions, and in this process ~240 lines had their log gfs selected among values from Sneden et al. (1996), Kupka et al. (1999; VALD), Biehl (1976), Steffen (1985), McWilliam & Rich (1994), and Bensby et al. (2003). Additionally, 21 hyperfine structures for the heavy elements Ba, La, Eu, Co, Pb were included, adopting a solar isotopic mix. For the hyperfine structures, a code described and made available by McWilliam (1998) was employed, as described in Allen (2005).

Accurate values for the damping constant γ are also important for computation of line profiles. This is crucial for the strong lines, and it also has a non-negligible effect on weaker lines (see Ryan 1998, for a discussion).

In our atomic line list, 36% of the lines had the collisional broadening obtained from Anstee & O'Mara (1995), Barklem & O'Mara (1997), Barklem et al. (1998), and Barklem et al. (2000) (this series of papers is referred to hereafter as ABO). Those lines correspond to the totality of the strong neutral lines. The other lines were either of higher ionization stages[1] or were not in the energy domain range of the tabulated cross sections. Thus these lines were either manually fitted to the Sun or were assumed to have interaction constant $C_6 = 0.3 \times 10^{-31}$.

Around 5% of the lines which had C_6 derived from ABO cross sections had to be manually fitted in order to reproduce the solar spectrum. This happened due to the dependence of the line profile both on the collisional broadening and on the model atmosphere employed. The conversion of the ABO cross sections into C_6 values are explained in Appendix A.

The high quality of the final line list can be assessed by comparisons with high resolution spectra of the Sun (Kurucz et al. 1984) and Arcturus (Hinkle et al. 2000). The resolution of these spectra are on the order $R \sim 10^5$, thus allowing a thorough verification of the accuracy of our wavelengths, oscillator strengths, and damping constants. In Figs. 1 and 2, comparisons of our synthetic spectra to those of the Sun and Arcturus are shown in two spectral regions. For the Sun the synthetic spectrum was computed adopting $T_{\rm eff}$ = 5770 K, log g = 4.44, microturbulent velocity $v_{\rm t}$ = 1.0 km s^{-1} and abundances from Grevesse & Sauval (1998). For Arcturus the adopted parameters were $T_{\rm eff}$ = 4275 K, log g = 1.55, and $v_{\rm t}$ = 1.65 km s^{-1} (Meléndez et al. 2003). An ATLAS9 model atmosphere with these parameters was kindly computed by F. Castelli (private comunication). For the abundances, we adopted [Fe/H] = −0.54, [C/Fe] = −0.08, [N/Fe] = +0.30, [O/Fe] = 0.43, and [Ni/Fe] = +0.02 from Meléndez et al. (2003), [Mg/Fe] = +0.30, and [Ca/Fe] = +0.17 from McWilliam & Rich (1994).

In both figures the Sun is reproduced very well. For the case of Arcturus, the synthetic spectrum looks somewhat strong-lined. At such high resolution, small errors in the atmospheric parameters can easily account for this difference, and the overall agreement is very good.

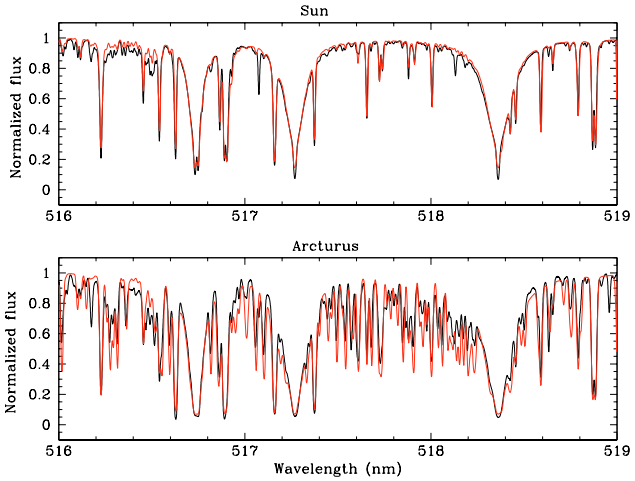

Fig. 1. *Upper panel*: comparison of the observed solar spectrum (thin line) and synthetic spectrum (thick line). *Lower panel*: comparison of Arcturus observed spectrum (thin line) and synthetic spectrum (thick line). Adopted parameters are given in the text.

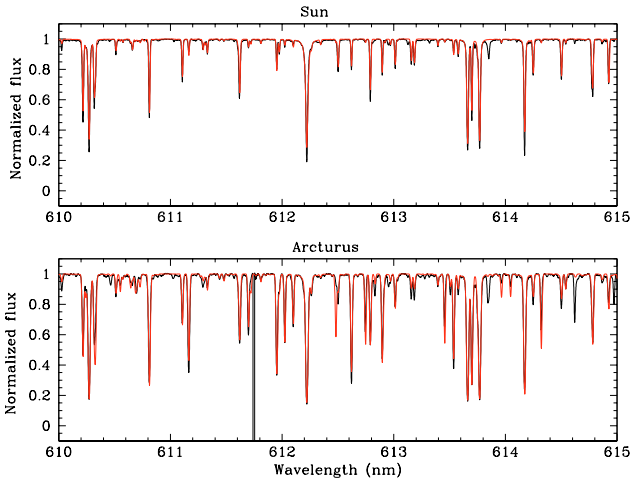

Fig. 2. Same as Fig. 1 for the region 610−615 nm.

[1] Cross sections for ionized lines are not easily computed (see Barklem & O'Mara 1998 and Barklem et al. 2000). The cross sections for ionized transitions presented in Barklem et al. (2000) were included in our line list.

Table 1. Molecules considered in the computations of the synthetic spectra. References: (1) Huber & Herzberg (1979); (2) Pradhan et al. (1994); (3) Schulz & Armentrout (1991);

Molecule	System	Number of lines	Wavelength coverage (nm)	Number of vibrational bands	Dissociation potential (ref) $D_\circ$ (eV)
MgH	$A^2\Pi$–$X^2\Sigma$	1945	404–609	13	1.34 (1)
C_2 Swan	$A^3\Pi$–$X^3\Pi$	11 254	429–676	35	6.21 (1)
CN blue	$B^2\Sigma$–$X^2\Sigma$	92 851	300–600	197	7.72 (2)
CN red	$A^2\Pi$–$X^2\Sigma$	23 828	404–2714	74	"
CH AX	$A^2\Delta$–$X^2\Pi$	10 137	321–786	20	3.46 (1)
CH BX	$B^2\Delta$–$X^2\Pi$	2016	361–682	10	"
CH CX	$C^2\Delta$–$X^2\Pi$	2829	270–424	12	"
CO nir	$X^1\Sigma^+$	7088	1578–5701	63	11.09 (1)
NH blue	$A^3\Pi$–$X^3\Sigma$	8599	300–600	55	3.47 (1)
OH blue	$A^2\Sigma$–$X^2\Pi$	6018	300–540	46	4.39 (1)
OH nir	$X^2\Pi$	2028	746–2594	43	"
FeH	$A^4\Delta$–$X^4\Delta$	2705	778–1634	9	1.63 (3)
TiO γ	$A^3\Phi$-$X^3\Delta$	26 007	622–878	23	6.87 (1)
TiO γ'	$B^3\Pi$–$X^3\Delta$	219 367	501–915	81	"
TiO α	$C^3\Delta$–$X^3\Delta$	360 725	380–861	79	"
TiO β	$c^1\Phi$–$a^1\Pi$	91 804	431–804	63	"
TiO δ	$b^1\Pi$–$a^1\Delta$	189 019	622–1480	66	"
TiO ϵ	$E^3\Pi$–$X^3\Delta$	253 755	641–1341	61	"
TiO ϕ	$b^1\Pi$–$d^1\Sigma$	105 082	665–1780	65	"

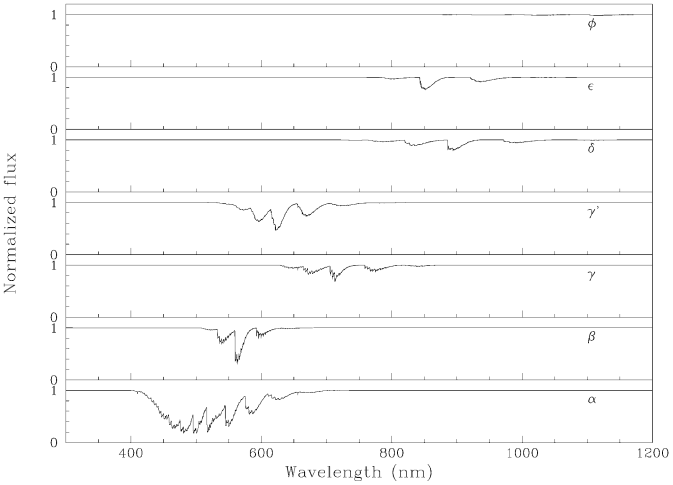

Fig. 3. Each of the seven TiO systems considered in this work, computed separately. The identification of each band is given in the figure. These spectra were computed with ($T_{\rm eff}$, log g, [Fe/H], [α/Fe]) = (3500, 0.0, 0.0, 0.0).

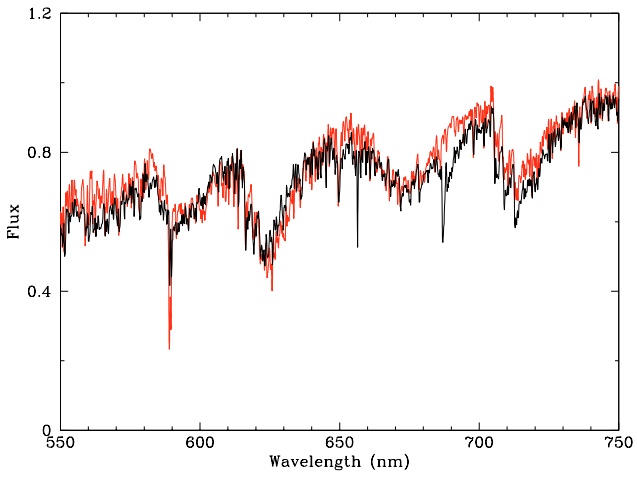

Fig. 4. Comparison between the star HD 102212 (thin line), atmospheric parameters ($T_{\rm eff}$, log g, [Fe/H]) = (3660, 0.0, 0.0), obtained from STELIB library, and a synthetic spectrum (thick line), parameters ($T_{\rm eff}$, log g, [Fe/H], [α/Fe]) = (3600, 0.0, 0.0, 0.0). This wavelength range illustrates the TiO γ and γ' systems.

When comparing synthetic spectrum with observed spectrum, one also has to be aware that observed spectra taken through the atmosphere include telluric lines, whereas computed spectra do not. A crucial aspect of our procedure is the derivation of reliable oscillator strengths from comparison with ground-based observations of the Sun and Arcturus, as explained in Barbuy et al. (2003). This, however, is not feasible in regions of the spectra which are heavily contaminated by telluric lines. For that reason, there is a gap in the line list between 1.35 and 1.50 μm – where the telluric absorption is severe – since we refrained from adopting lines with purely theoretical log gfs in that region.

2.2. Molecular line opacities

Molecular lines are an important source of opacity in the atmospheres of late-type stars. Molecular bands in fact dictate the overall shape of the spectra of late-K and M stars, which are the dominant contributors to the integrated light of old and intermediate-age stellar populations longward of ~650 nm. Therefore, it is crucial to model their intensities correctly if one wants to make accurate predictions in these spectral regions. The molecules considered in the calculation of the present library are listed in Table 1.

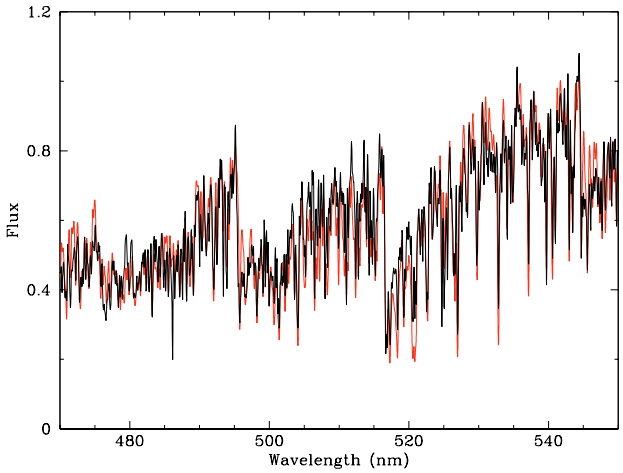

Fig. 5. Comparison between the star HD 39801 (thin line), atmospheric parameters ($T_{\rm eff}$, log g, [Fe/H]) = (3540, 1.0, 0.0), obtained from Indo-US library, and a synthetic spectrum (thick line), parameters ($T_{\rm eff}$, log g, [Fe/H], [α/Fe]) = (3600, 1.0, 0.0, 0.0). This wavelength range illustrates the TiO α system.

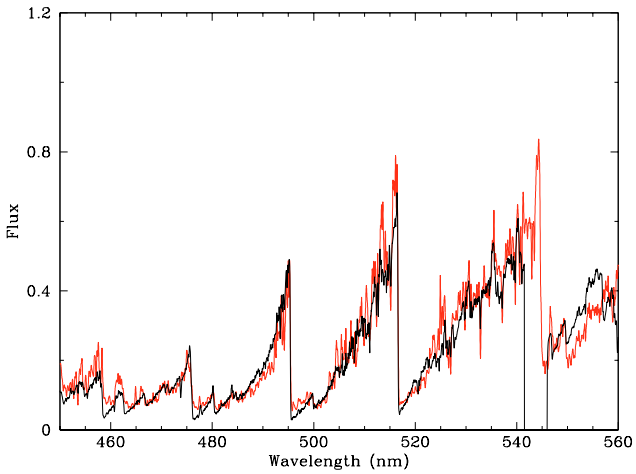

Fig. 6. Comparison between the star HD 126327 (thin line), atmospheric parameters ($T_{\rm eff}$, log g, [Fe/H]) = (3000, 0.0, −0.58), obtained from Indo-US library, and a synthetic spectrum (thick line), parameters ($T_{\rm eff}$, log g, [Fe/H], [α/Fe]) = (3000, 0.0, 0.0, 0.0). This wavelength range illustrates the TiO α system.

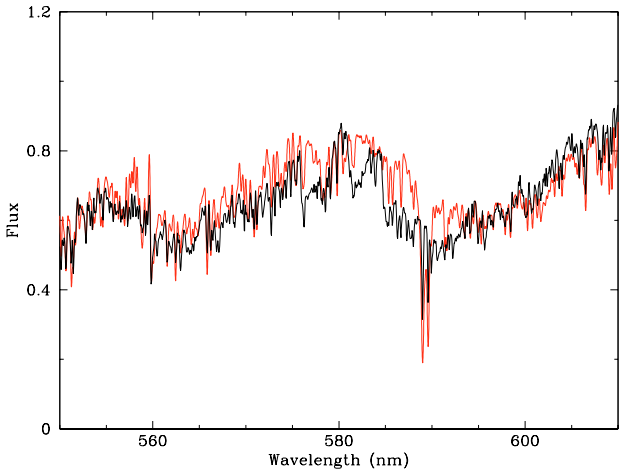

Fig. 7. Comparison between the star HD 217906 (thin line), atmospheric parameters ($T_{\rm eff}$, log g, [Fe/H]) = (3600, 1.2, −0.11), obtained from Indo-US library, and a synthetic spectrum (thick line), parameters ($T_{\rm eff}$, log g, [Fe/H], [α/Fe]) = (3600, 1.0, 0.0, 0.0). This wavelength range illustrates basically the TiO β system.

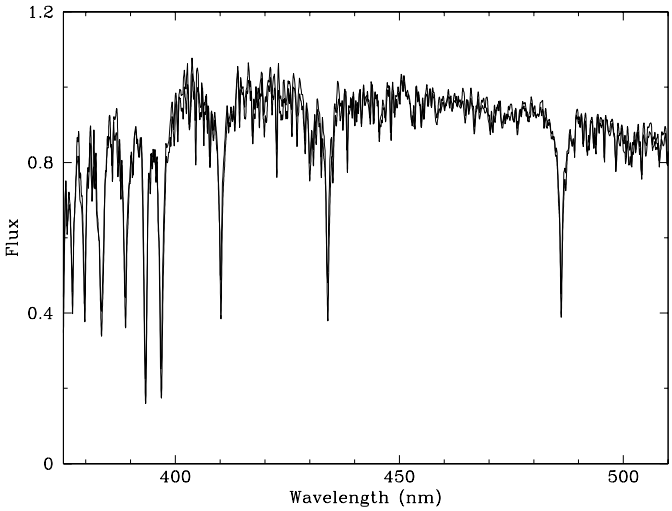

Fig. 8. Comparison between the star HD 126141 (thin line), spectral type F5V, and atmospheric parameters ($T_{\rm eff}$, log g, [Fe/H]) = (6670, 4.3, −0.02), obtained from STELIB library, and a synthetic spectrum (thick line), parameters ($T_{\rm eff}$, log g, [Fe/H], [α/Fe]) = (6750, 4.5, 0.0, 0.0).

The line list for the molecules MgH, C_2, and CN-red were adopted from Balfour & Cartwright (1976), Phillips & Davis (1968), and Davis & Philips (1963), respectively. For the CN-blue, NH, and OH-blue systems, the line lists by Kurucz (1993) were adopted, as implemented in Castilho et al. (1999). For the CH blue systems, the LIFBASE program of Luque & Crosley (1999) was used. The OH vibration-rotation line list is the one implemented in Meléndez et al. (2001). It is based on the laboratory work of Abrams et al. (1994), complemented with the theoretical line list by Goldman et al. (1998). The molecular gf-values of the OH lines were obtained from the Einstein coefficients calculated by Goldman et al. (1998). The CN and CO infrared line lists were implemented in Meléndez & Barbuy (1999). The CO lines are from the theoretical work of Goorvitch (1994), and the infrared CN lines are from S. P. Davis, based on the analyses by M. L. P. Rao (S. P. Davis, private communication). The FeH ($A^4\Delta$-$X^4\Delta$) line list of rotational lines was adopted from Philips et al. (1987), as described in Schiavon et al. (1999). The dissociation potential values adopted for all molecules are reported in Table 1, together with corresponding sources.

The line list for the TiO γ system was adopted from the theoretical work by Jorgensen (1994). The electronic oscillator strength was calibrated to the intensity of the laboratory line list used in Erdelyi-Mendes & Barbuy (1989). For the remaining TiO electronic systems, the list by Plez (1998) was adopted.

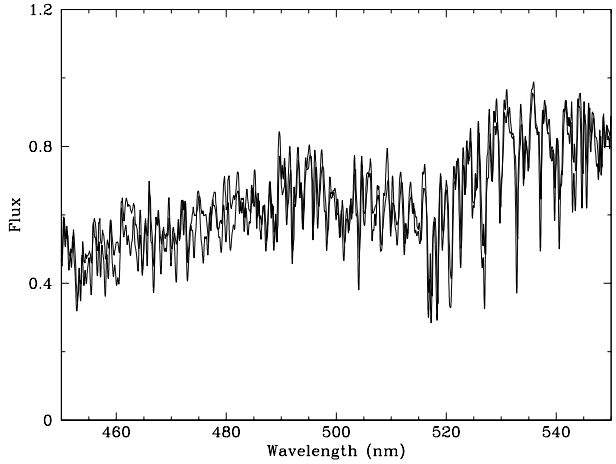

Fig. 9. Comparison between the star HD 148513 (thin line), spectral type K4III, and atmospheric parameters ($T_{\rm eff}$, log g, [Fe/H]) = (3979, 1.03, −0.14), obtained from STELIB library, and a synthetic spectrum (thick line), parameters ($T_{\rm eff}$, log g, [Fe/H], [α/Fe]) = (4000, 1.0, 0.0, 0.0).

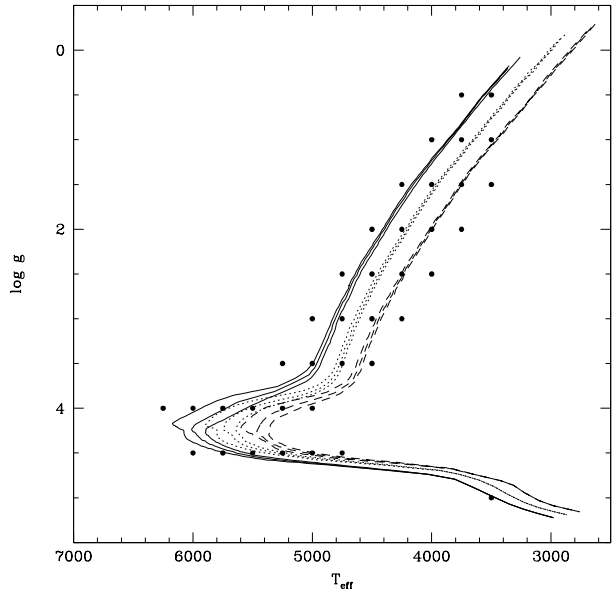

Fig. 10. Bertelli et al. (1994) isochrones for three metallicities ([Fe/H] = −0.4, 0.0, +0.4; solid, dotted and dashed lines), and three ages (8, 10.5, and 13 Gyr; from left to right). The circles indicate the extension of the α-enhanced main grid, computed with [α/Fe] = 0.4, [Ca/Fe] = 0.0 and [Fe/H] = (−0.5, 0.0, 0.2 and 0.5).

The Plez line list contains several million lines, which makes the computations extremely time-consuming, so that we decided to eliminate very weak lines in order to speed up our calculations. Therefore, we include only the lines which simultaneously satisfy the following set of conditions: log $gf \geq -4.0$, $J'' \leq 120$, and v', $v'' \leq 9$, where J'' is the rotational quantum number of the lower level of the transition and v', and v'' are the vibrational quantum numbers of the upper and lower levels of the transition. These values were chosen after several tests were performed, in order to make sure that removal of lines not satisfying these criteria would have a negligible impact on our computations.

The electronic oscillator strengths ($f_{\rm el}$) for the TiO systems were obtained empirically by matching band strengths in spectra of observed cool stars with our synthetic spectra. For this purpose, cool giants covering the effective temperature range $3000 \leq T_{\rm eff} \leq 3800$ K were selected from the STELIB and Indo-US libraries. In this temperature range, TiO bands dominate the line opacity in the visible region of the spectra of M giants. Because the model atmospheres by Castelli & Kurucz (2003) do not go below $T_{\rm eff} = 3500$ K, we employed MARCS model atmospheres from Plez et al. (1992) to calibrate these $f_{\rm el}$.

In Fig. 3 the relative contribution of each of the TiO systems, calculated for a cool giant, is presented. Some comparisons between empirically calibrated TiO-dominated synthetic spectra to the spectra of some observed stars are presented in Figs. 4 to 7. Moreover, comparison to the spectra of an F dwarf and a K giant is presented in Figs. 8 and 9, respectively. The wavelength range plotted in the latest two figures were chosen to illustrate the spectral region where those spectral types dominate the flux of integrated population spectra. The synthetic spectra shown in these figures are the ones whose atmospheric parameters are the closest to those of the observed stars, as given in the respective library (STELIB or Indo-US).

In all figures from 4 to 9 the synthetic spectra were convolved to match the different resolutions of the observed spectra (*FWHM* ≈ 1 Å for Indo-US and ≈3 Å for STELIB).

3. Library of synthetic spectra

Given the atomic and molecular line lists described in the previous section, a library of synthetic spectra was computed from 3000 Å to 1.8 μm, in steps of 0.02 Å. The model atmosphere grid is available for microturbulent velocities $v_{\rm t} = 2$ km s^{-1}, but the synthetic spectra were calculated with values more representative of the observed stars as given below:

- $v_{\rm t} = 1.0$ km s^{-1} for log $g \geq 3.0$;
- $v_{\rm t} = 1.8$ km s^{-1} for $1.5 \leq$ log $g \leq 2.5$, and;
- $v_{\rm t} = 2.5$ km s^{-1} for log $g \leq 1.0$.

The output of the synthesis code is normalised flux. In order to produce spectra in an absolute flux scale, the normalised high-resolution spectra were multiplied by the true continuum given directly by the ATLAS9 model atmosphere. The library is presented in both normalized and absolute flux formats and is available in FITS format upon request to the authors, or in ASC format at the CDS.

3.1. Coverage in stellar parameter space

The main grid covers the following parameters:

- Effective temperatures: $3500 \leq T_{\rm eff} \leq 7000$ K in steps of 250 K.
- Surface gravities: $0.0 \leq$ log $g \leq 5.0$ in steps of 0.5.
- Metallicities: [Fe/H] = −2.5, −2.0, −1.5, −1.0, −0.5, 0.0, 0.2 and 0.5.
- Chemical compositions: [α/Fe] = 0.0 and 0.4, where the α-elements considered are O, Ne, Mg, Si, S, Ca and Ti.

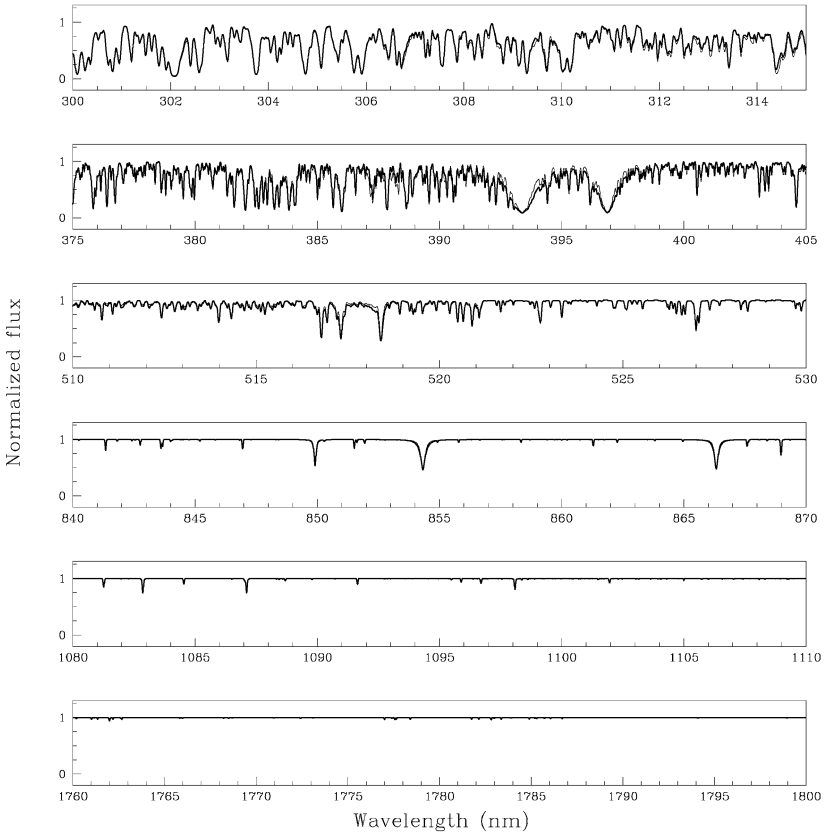

Fig. 11. Solar scaled (thin line) and α-enhanced (thick line) synthetic spectrum computed with $T_{\rm eff}$ = 4500 K, log g = 3.0, and [Fe/H] = −2.0 for different wavelength regions. The spectra were convolved to *FWHM* ∼ 0.5 Å.

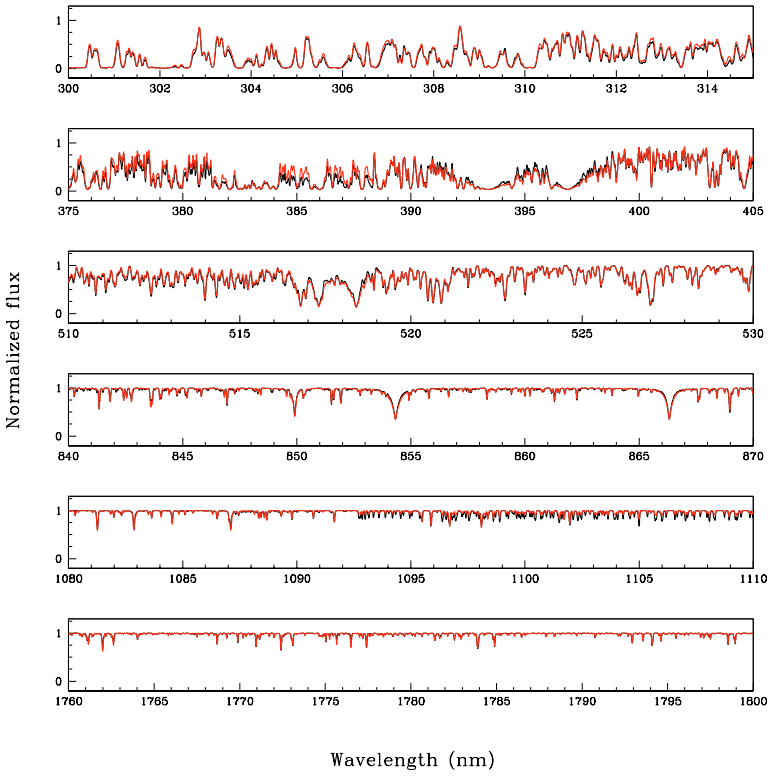

Fig. 12. Solar scaled (thin line) and α-enhanced (thick line) synthetic spectrum computed with $T_{\rm eff}$ = 4500 K, log g = 3.0, and [Fe/H] = 0.0 for different wavelength regions. The spectra were convolved to *FWHM* ∼ 0.5 Å.

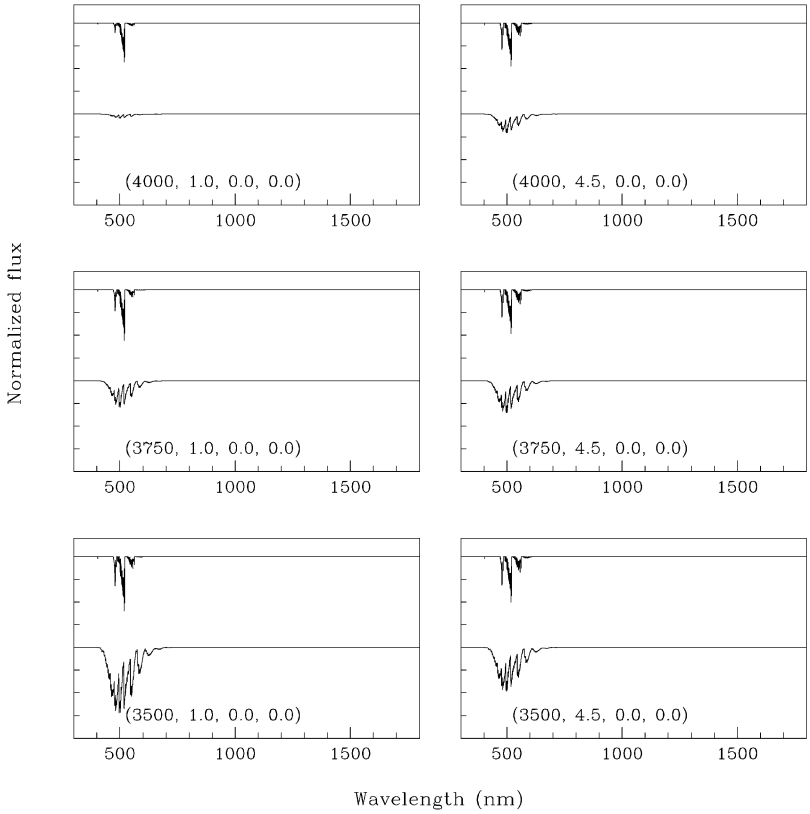

Fig. 13. Individual contribution of the MgH and TiO α molecules for three $T_{\rm eff}$ and two log g (indicated in the figures). The top plot in each panel represents the MgH spectrum, and the bottom plot presents the TiO α spectrum.

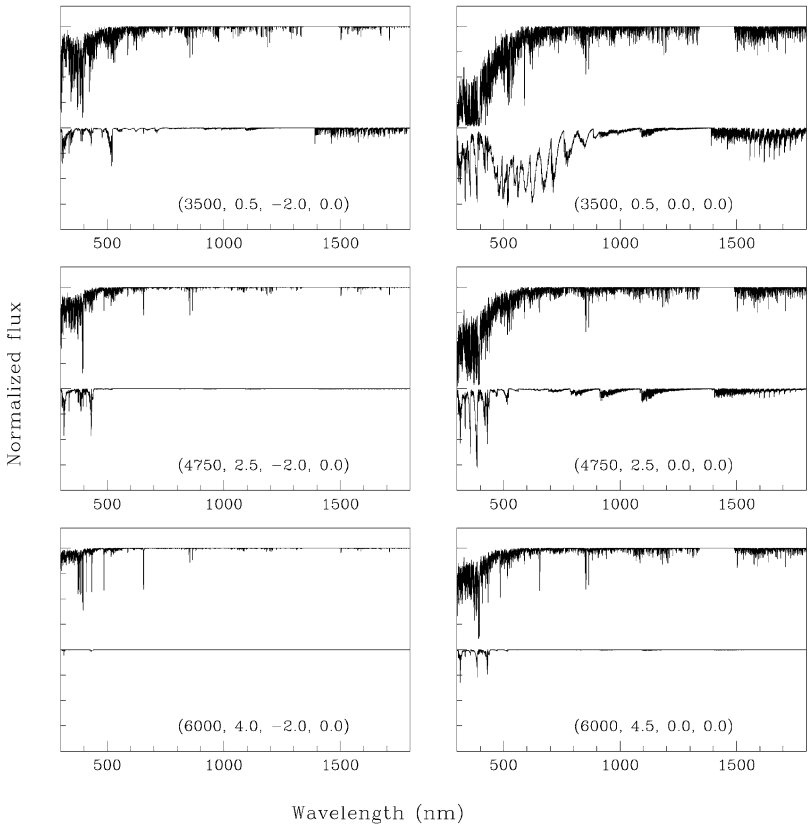

Fig. 14. The relative contribution of atomic and molecular line opacities for six combinations of ($T_{\rm eff}$, log g, [Fe/H], [α/Fe]) as indicated in each panel. The top spectrum of each panel shows the normalised atomic contribution (an offset was applied) and the lower spectrum shows the normalised molecular contribution.

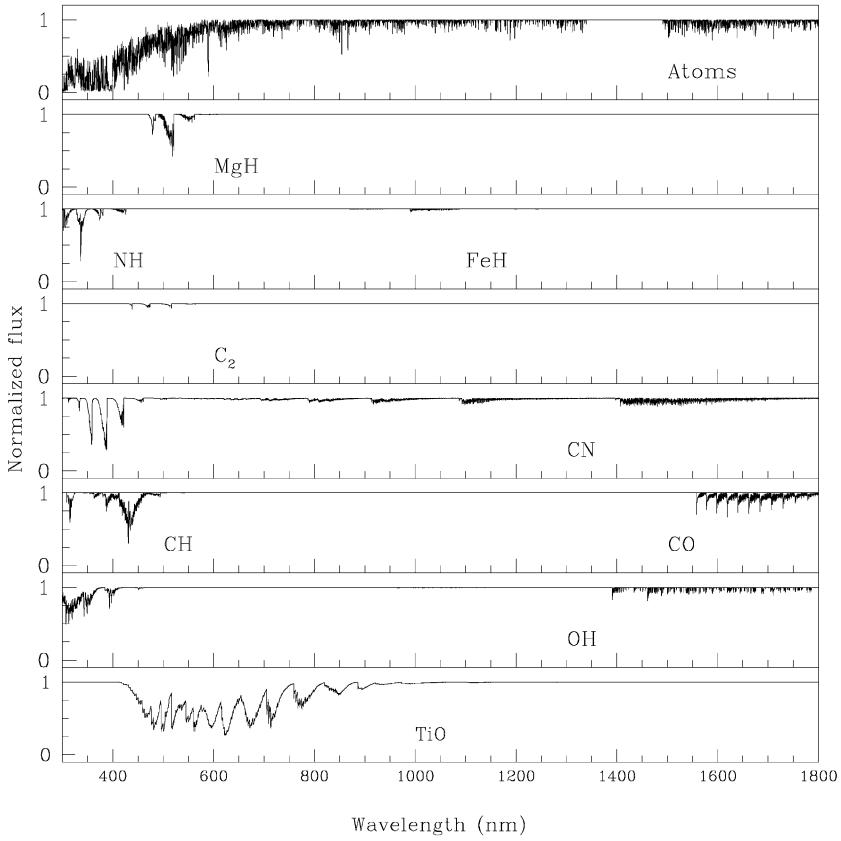

Fig. 15. Individual contribution from each molecule for the parameters ($T_{\rm eff}$, log g, [Fe/H], [α/Fe]) = (3500, 0.5, 0.0, 0.0). The molecules considered are labeled in each panel.

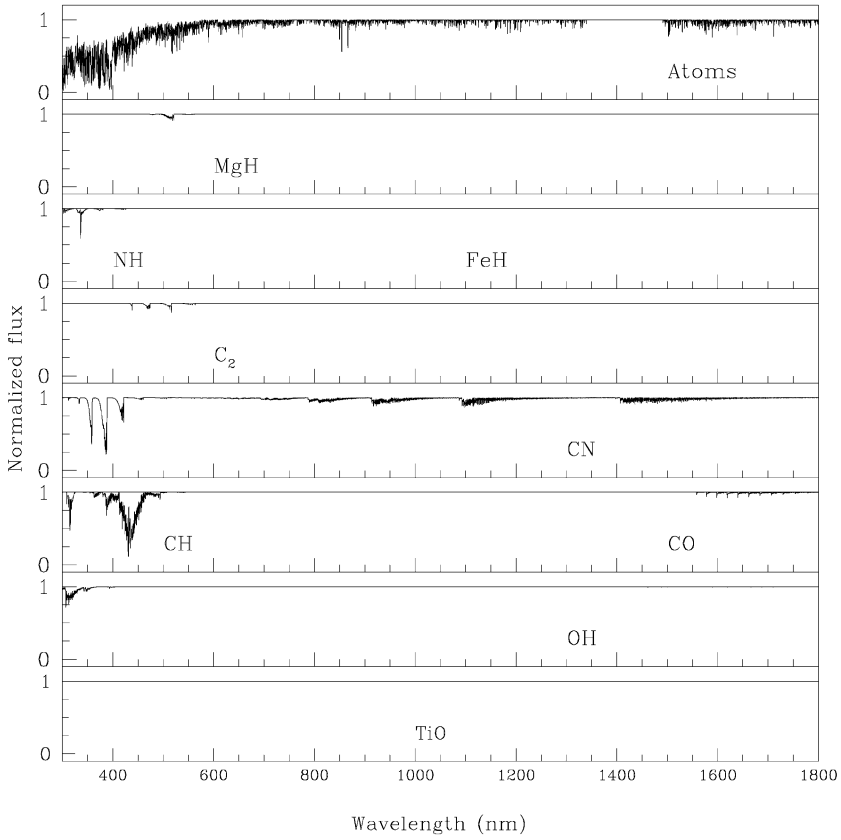

Fig. 16. Same as Fig. 15 for ($T_{\rm eff}$, log g, [Fe/H], [α/Fe]) = (4750, 2.5, 0.0, 0.0).

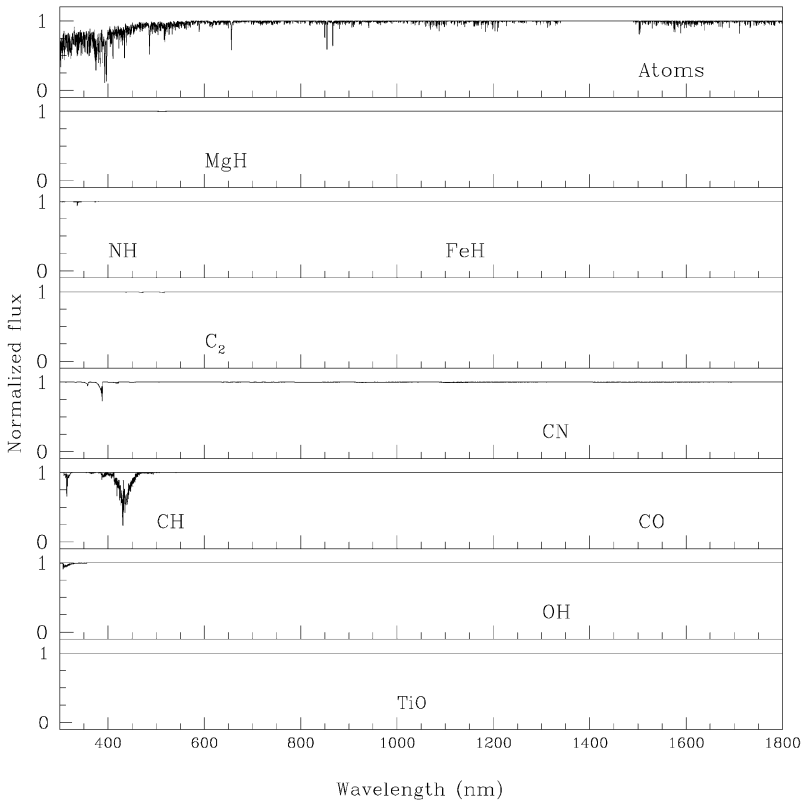

Fig. 17. Same as Fig. 15 for ($T_{\rm eff}$, log g, [Fe/H], [α/Fe]) = (6000, 4.0, 0.0, 0.0). Only the molecules CH and CN have non-negligible effects in the total spectrum.

It has not been well established yet whether titanium is associated to the synthesis of the α-elements or to the iron-peak elements (Timmes et al. 1995). Nevertheless, it has been shown that its abundance follows the same pattern as that of α-elements for several types of populations (e.g. McWilliam & Rich 1994; Pompéia et al. 2003), and thus we decided to include this element in the α-enhanced group.

Concerning calcium, observations of halo and disk Galactic stars show that [Ca/Fe] closely follows the behaviour of other α-elements as a function of [Fe/H] (McWilliam & Rich 1994; Edvardsson et al. 1993). In the bulge of our galaxy, however, some high-resolution analyses show that [Ca/Fe] seems to be close to solar (e.g. Zoccali et al. 2004). From lower resolution studies, there is evidence as well that [Ca/Fe] is not enhanced in elliptical galaxies (e.g. Thomas et al. 2003b), although Prochaska et al. (2005) show that the calcium abundance derived from the Ca4227 index is dependent on the index-measuring strategy.

Considering the application of this grid to the study of old and metal-rich stellar populations, a subsample of the α-enhanced main grid was also computed with [Ca/Fe] = 0.0, for [Fe/H] = −0.5, 0.0, 0.2, and 0.5. The sets of $T_{\rm eff}$ and log g for these computations were chosen amongst those that are relevant for old stellar populations at these metallicities, for ages between 8 and 13 Gyr. Bertelli et al. (1994) isochrones were used to guide our selection. Some of these isochrones are presented in Fig. 10 as well as the ($T_{\rm eff}$, log g) pairs computed for this extension of the library.

High resolution synthetic spectra computed for a cool giant with solar-scaled and α-enhanced abundance patterns are compared in Figs. 11 and 12, for the metal-poor and metal-rich cases, respectively. As expected, well-known indicators of abundances of α-elements, such as the Mg triplet lines at 517 nm, the MgH band at 518 nm and the Ca triplet in the far red, are stronger in the α-enhanced spectra. We note, however, other lines which are very sensitive to α-enhancement and yet are virtually unexplored in work on stellar populations (e.g. the Ca H & K lines and the lines due to the CN molecule, at $\lambda > 1093$ nm). We also note that some lines are visibly weaker in the α-enhanced case (e.g. the region around 385 nm in Fig. 12). This cannot be attributed to individual abundance variations of the non-α elements, because those abundances are the same as in the solar scaled case. The decrease in the intensity of some lines can be explained because the α-elements, especially Mg, are electron donors and thus contribute in an important way to the continuum opacity. Because the spectra shown in Figs. 11 and 12 are normalised, the net effect is that some lines in the α-enhanced case look weaker due to enhanced continuum opacity, even when the individual abundances corresponding to those lines are unchanged.

3.2. The relative contribution of different chemical species to the total line opacity

A great advantange of synthetic spectra over observed spectra is that with spectral synthesis it is possible to disentangle the relative contribution of different chemical species to the line

spectrum, which allows more careful study of line indices. For example, it is possible to evaluate the presence of blends or the range of applicability of a given line indice.

As an example, the well-known Lick indices Mg_1, Mg_2, and Mg_b measure the intensity of the MgI triplet lines (5167.327, 5172.698 and 5183.619 Å) together with MgH, C_2, and TiO bands, besides other atomic lines. These indices essentially measure MgI and MgH in K giants and in the integrated light of galaxies. However, it should be noted that in stars cooler than 3750 K, bands from the α system of TiO become stronger than MgH, as can be seen in Fig. 13. It is clear that for very metal-rich stars at the tip of the red giant branch and galaxies containing such stars, these indices are substantially affected by TiO bands, which makes their interpretation somewhat more complicated (see also Schiavon 2005).

The separate contribution of atoms and molecules is shown in Fig. 14 for the parameters ($T_{\rm eff}$, log g) = (3500, 0.5), (4750, 2.5) and (6000, 4.0) for [Fe/H] = -2.0 and 0.0 ([α/Fe] = 0.0). In order to illustrate the contribution of atoms and each diatomic molecule, we computed each molecule separately. The results are shown in Figs. 15–17, where the impact of each molecule on the line spectrum can be evaluated.

4. Summary

A library of synthetic stellar spectra is presented. This library was computed with a sampling 0.02 Å and for the parameters: effective temperatures $3500 \leq T_{\rm eff} \leq 7000$ K, surface gravities $0.0 \leq \log g \leq 5.0$, metallicities $-2.5 \leq$ [Fe/H] $\leq +0.5$, and α-elements over Fe ratio [α/Fe] = 0.0 and 0.4. For the metallicites [Fe/H] ≥ -0.5, two α-enhanced grids are available, with and without Ca in the enhanced group.

For the computation of this grid, an atomic line list was implemented based on the previous lists of Barbuy et al. (2003) and Meléndez & Barbuy (1999). The log gf values were updated to the most recent NIST values, and damping constants were calculated for the totality of strong lines following ABO papers.

The molecular line opacities include the molecules MgH, C_2, CN, CH, CO, OH, NH, FeH, and TiO. The TiO systems, which dominate the opacity of cool stars in the visible wavelength range, were calibrated by comparison with observed stars in the empirical libraries STELIB and Indo-US.

This high-resolution stellar synthetic library simultaneosly covers a wide wavelength range and α-enhanced chemical compositions. The α-enhancement, in particular, is indispensable to the reproduction of the integrated properties of old stellar populations, for all metallicities regimes. This library is a valuable and powerful tool for the study of stellar populations, and can be used to model old metal-rich stellar populations with unprecedented accuracy.

Note added in proof We would like to mention that by the time of the acceptance of our paper, two recent libraries including variable α-enhancement came to our knowledge, Munari et al. (2005) and Brott & Hauschild (2005).

Acknowledgements. We are grateful to the referee Robert Kurucz for his comments, Roger Cayrel for valuable discussions on collisional broadening, and Dinah M. Allen for the heavy-elements line list. P.C. acknowledges: a Fapesp PhD fellowship No. 2000/05237-9; the Latin American-European Network on Astrophysics and Cosmology (LENAC) of the European Union's ALFA Programme; and Fiorella Castelli, for help with the ATLAS model atmospheres. BB acknowledges partial financial support from CNPq and Fapesp. R.P.S. acknowledges financial support from HST Treasury Program grant GO-09455.05-A to the University of Virginia.

References

Abrams, M. C., Davis, S. P., Rao, M. L. P., & Engleman, R., Jr. 1994, ApJS, 93, 351
Allard, F., & Hauschildt, P. H. 1995, ApJ, 445, 433
Allen, D. M. 2005, Ph.D. Thesis, Univ. de São Paulo
Anstee, S. D., & O'Mara, B. J. 1991, MNRAS, 253, 549
Anstee, S. D., & O'Mara, B. J. 1995, MNRAS, 276, 859
Barbuy, B. 1982, Ph.D. Thesis, Université de Paris VII
Barbuy, B., Perrin, M.-N., Katz, D., et al. 2003, A&A, 404, 661
Balfour, W. J., & Cartwright, H. M. 1976, A&AS, 26, 389
Barklem, P. S., & O'Mara, B. J. 1997, MNRAS, 290, 102
Barklem, P. S., & O'Mara, B. J. 1998, MNRAS, 300, 863
Barklem, P. S., O'Mara, B. J., & Ross, J. E. 1998, MNRAS, 296, 1057
Barklem, P. S., Piskunov, N., & O'Mara, B. J. 2000, A&AS, 142, 467
Bell, R. A., Dwivedi, P. H., Branch, D., & Huffaker, J. N. 1979, ApJS, 41, 593
Bensby, T., Feltzing, S., & Lundstrom,öI. 2003, A&A, 410, 527
Bertelli, G., Bressan, A., Chiosi, C., Fagotto, F., & Nasi, E. 1994, A&AS, 106, 275
Bessell, M. S. 1991, A&AS, 89, 335.
Bessell, M. S., Brett, J. M., Wood, P. R., & Scholz, M. 1989, A&AS, 77, 1
Biehl, D. 1976, Ph.D. Thesis, Univ. Kiel
Brott, I., & Hauschildt, P. H. 2005, in The Three Dimensional Universe with Gaia, ed. M. A. C. Perryman and C. Turon, ESA SP-576, 565
Bruecknerm K. 1971, ApJ, 169, 621
Bruzual, A. G., & Charlot, S. 1993, ApJ, 405, 538
Bruzual, A. G., & Charlot, S. 2003, MNRAS, 344, 1000
Burstein, D., Faber, S. M., Gaskell, C. M., & Krumm, N. 1984, ApJ, 287, 56
Buzzoni, A. 2002, AJ, 123, 1188
Castelli, F., & Kurucz, R. L. 2003, Proc. of the 210th Symposium of the International Astronomical Union held at Uppsala University, Uppsala, Sweden, 17−21 June, 2002. ed. N. Piskunov, W. W. Weiss, and D. F. Gray. Published on behalf of the IAU by the Astronomical Society of the Pacific 2003, A20
Castilho, B. V., Spite, F., Barbuy, B., et al. 1999, A&A, 345, 249
Cayrel, R., Perrin, M. N., Buser, R., Barbuy, B., & Coupry, M. F. 1991a, A&A, 247, 122
Cayrel, R., Perrin, M.-N., Barbuy, B., & Buser, R. 1991b, A&A, 247, 108
Cayrel, R., Faurobert-Scholl, M., Feautrier, N., Spielfieldel, A., & Thevenin, F. 1996, A&A, 312, 549
Cerviño, M., & Mas-Hesse, J. 1994, A&A, 284, 749
Chavez, K., Malagnini, M. L., & Morossi, C. 1997, A&AS, 126, 267
Davis, S. P., & Phillips, J. G. 1963, Berkeley Analyses of Molecular Spectra (Berkeley: University of California Press)
Delgado, R. M. González, Cerviño, M., et al. 2005, MNRAS, 357, 945
Erdelyi-Mendes, M., & Barbuy, B. 1989, A&AS, 80, 229

Edvardsson, B., Andersen, J., Gustafsson, B., et al. 1993, A&A, 275, 101
Fioc, K., & Rocca-Volmerange, B. 1997, A&A, 326, 950
Fluks, M. A., Plez, B., The, P. S., et al. 1994, A&AS, 105, 311
Franchini, M., Morossi, C., Di Marcantonio, P., et al. 2004, ApJ, 601, 485
Fuhrmann, K., Axer, M., & Gehren, T. 1993, A&A, 271, 451
Girard, P., & Soubiran, C. 2005, Proc. of the Gaia Symposium, The Three-Dimensional Universe with Gaia (ESA SP-576). Held at the Observatoire de Paris-Meudon, 4−7 October 2004, ed. C. Turon, K. S. O'Flaherty, M. A. C. Perryman, 169
Goldman, A., Shoenfeld, W. G., Goorvitch, D., et al. 1998, JQSRT, 59, 453
Gray, D. 1976, The observation and analysis of stellar photospheres (New York: Wiley-Interscience)
Grevesse, N., & Sauval, A. J. 1998, Space Sci. Rev., 85, 161
Goorvitch, D. 1994, ApJS, 95, 535
Gunn, J. E., & Stryker, L. L. 1983, ApJS, 52, 121
Heavens, A., Panter, B., Jimenez, R., & Dunlop, J. 2004, Nature, 428, 625
Hinkle, K., Wallace, L., Valenti, J., & Harmer, D. 2000, Visible and Near Infrared Atlas of the Arcturus Spectrum 3727−9300 A, ed. K. Hinkle, L. Wallace, J. Valenti, and D. Harmer (San Francisco: ASP)
Holweger, H., & Müller, E. 1974, Sol. Phys., 39, 19 (HM74)
Huber, K. P., & Herzberg, G. 1979, Constants of Diatomic Molecules, van Nostrand Reinhold, New York Spectra of Diatomic Molecules (Am. Elsevier Pub. Co.)
Jacoby, G. H., Hunter, G. A., & Christian, C. A. 1984, ApJ, 419, 592
Jimenez, R., MacDonald, J., Dunlop, J., Padoan, P., & Peacock, J. 2004, MNRAS, 349, 240
Jones, L. A. 1999, Ph.D. Thesis, University of North Carolina, Chapel Hill
Jorgensen, U. G. 1994, A&A, 284, 179
Katz, D., The Rvs Team 2004, Semaine de l'Astrophysique Francaise, meeting held in Paris, France, ed. F. Combes, D. Barret, T. Contini, F. Meynadier & L. Pagani (EdP-Sciences, Conf. Ser.)
Kupka, F., Piskunov, N., Ryabchikova, T. A., Stempels, H. C., & Weiss, W. W. 1999, A&AS, 138, 119
Kurucz, R. L. 1993, CD-ROM 13, 14, 18, 23
Kurucz, R. L., Furenlid, I., & Brault, J. 1984, Solar flux atlas from 296 to 1300 nm, National Solar Observatory Atlas, Sunspot (New Mexico: National Solar Observatory)
Le Borgne, J.-F., Bruzual, G., Pelló, R., et al. 2003, A&A, 402, 433
Leitherer, C., Schaerer, J., Goldader, J., et al. 1999, ApJS, 123, 3
Lejeune, Th., Cuisinier, F., & Buser, R. 1997, A&AS, 125, 229
Lejeune, Th., Cuisinier, F., & Buser, R. 1998, A&AS, 130, 65
Luque, J., & Crosley, D. R. 1999, SRI International Report MP 99-009
Maraston, C. 2005, MNRAS, submitted [arXiv:astro-ph/0410207]
McWilliam, A. 1997, ARA&A, 35, 503
McWilliam, A. 1998, AJ, 115, 1640
McWilliam, A., & Rich, R. M. 1994, ApJS, 91, 749
Martins, L., Gonzalez Delgado, R. M., Leitherer, C., Cerviño, M., & Hauschildt, P. 2005, MNRAS, 358, 49
McWilliam, A., & Rich, R. M. 1994, ApJS, 91, 749
McWilliam, A., & Rich, R. M. 2004, Origin and Evolution of the Elements, from the Carnegie Observatories Centennial Symposia. Carnegie Observatories Astrophysics Series, ed. A. McWilliam and M. Rauch, Pasadena: Carnegie Observatories
Meléndez, J., & Barbuy, B. 1999, ApJS, 124, 527
Meléndez, J., & Barbuy, B. 2002, ApJ, 575, 474
Meléndez, J., Barbuy, B., & Spite, F. 2001, ApJ, 556, 858
Meléndez, J., Barbuy, B., Bica, E., et al. 2003, A&A, 411, 417
Mendes de Oliveira, C., Coelho, P., Gonzalez, J. J., & Barbuy, B. 2005, AJ, 130, 55
Munari, U., Castelli, F., & Zwitter, T. 2005, A&A, 442, 1127
Murphy, T., & Meiksin, A. 2004, MNRAS, 351, 1430
O'Mara, B. 1976, MNRAS, 177, 551
Panter, B., Heavens, A., & Jimenez, R. 2004, MNRAS, 355, 764
Pickles, A. J. 1998, PASP, 110, 863
Plez, B. 1998, A&A, 337, 495
Plez, B., Brett, J. M., Nordlund 1992, A&A, 256, 551
Phillips, J. G., & Davis, S. P. 1968, Berkeley Analyses of Molecular Spectra (Berkeley: University of California Press)
Phillips, J. G., Davis, S. P., Lindgren, B., & Balfour, W. J. 1987, ApJS, 65, 721
Pompéia, L., Barbuy, B., & Grenon, M. 2003, ApJ, 592, 1173
Praderie, F. 1967, Annales d'Astrophysique, 30, 31
Pradhan, A. D., Partridge, H., & Bauschlicher, C. W. J. 1994, J. Chem. Phys., 101, 3857
Prochaska, L. C., Rose, J. A., & Schiavon, R. P. 2005, AJ, submitted
Proctor, R. N., Forbes, D. A., & Beasley, M. A. 2004, MNRAS 355, 1327
Reader, J., Wiese, W. L., Martin, W. C., Musgrove, A., & Fuhr, J. R. 2002, NASA Laboratory Astrophysics Workshop, held May 1−3, 2002 at NASA Ames Research Center, Moffett Field, CA 94035-1000. Publisher: NASA, ed. F. Salama, Reference Conference Proceedings: NASA/CP-2002-21186, 80
Rodriguez-Merino, L. H., Chavez, M., Bertone, E., & Buzzoni, A. 2005, ApJ, 626, 411
Ryan, S. G. 1998, A&A, 331, 1051
Schiavon, R. P., Barbuy, B., & Singh, P. D. 1997, ApJ, 484, 499
Schiavon, R. P., & Barbuy, B. 1999, ApJ, 510, 934
Schiavon, R. P. 2005, ApJS, submitted
Schulz, R. H., & Armentrout, P. B. 1991, J. Chem. Phys., 94, 2262
Schulz, J., Fritze-v. Alvensleben, U., Möller, C. S., & Fricke, K. J. 2002, A&A, 392, 971
Sneden, C., McWilliam, A., Preston, G. W., et al. 1996, ApJ, 467, 819
Spielfiedel, A., Feautrier, N., Chambaud, G., & Levy, B. 1991, J. Phys. B: Atomic, Molecular, and Optical Physics, 24, 4711
Spite, M. 1967, Ann. d'Astroph., 30, 211
Steffen, M. 1985, A&AS, 59, 403
Steinmetz, M. 2003, ASPC, 298, 381
Tantalo, R., & Chiosi, C. 2004, MNRAS, 353, 917
Thomas, D., Maraston, C., & Bender, R. 2003a, MNRAS, 339, 897
Thomas, D., Maraston, C., & Bender, R. 2003b, MNRAS, 343, 279
Timmes, F. X., Woosley, S. E., & Weaver, T. A. 1995, ApJS, 98, 617
Trager, S. C., Worthey, G., Faber, S. M., Burstein, D., & González, J. J. 1998, ApJS, 116, 1
Tsuji, T. 1973, A&A, 23, 411
Unsold, A. 1955, Physik der Sternatmospharen, MIT besonderer Berucksichtigung der Sonne (Berlin: Springer)
Valdes, F., Gupta, R., Rose, J., Singh, H., & Bell, D. 2004, ApJS, 152, 251
Valenti, J. A., & Fischer, D. A. 2005, ApJS, 159, 141
van 't Veer-Menneret, C., & Megessier, C. 1996, A&A, 309, 879
Vazdekis, A. 1999, ApJ, 513, 224
Westera, P., Lejeune, T., Buser, R., Cuisinier, F., & Bruzual, G. 2002, A&A, 381, 524
Willemsen, P.G, Hilker M., Kayser, A., & Bailer-Jones, C. A. L. 2005, A&A, 436, 379
Worthey, G., Faber, S. M., & Gonzalez, J. J. 1992, ApJ, 398, 69
Worthey, G., Faber S. M., González, J. J., & Burstein, D. 1994, ApJS, 94, 687
Zoccali, M., Barbuy, B., Hill, V., et al. 2004, A&A, 423, 507
Zwitter, T., Castelli, F., & Munari, U. 2004, A&A, 417, 1055

Online Material

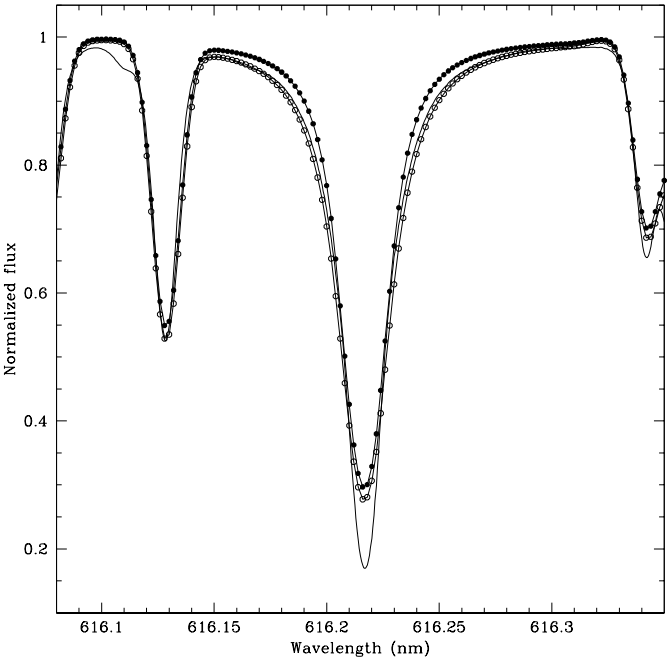

Fig. A.1. Comparison between the solar spectrum (solid line, no symbols) and synthetic spectrum calculated with ATLAS9 (solid line, open symbols) and HM74 (solid line, filled symbols) model atmospheres around the Ca 6162 Å line. The same parameters were adopted for the atomic transition considered in both calculations, and thus the difference in the line profiles is due only to the different model atmospheres employed.

Appendix A: Calculation of collisional broadening

The main source of collisional broadening for metallic lines in stars of spectral types between F and M is collisions with neutral hydrogen. The spectral synthesis code evaluates γ for each atmospheric layer given the interaction constant C_6:

$$\gamma_6/N_{\rm H} = 17 v^{3/5} C_6^{2/5}, \tag{A.1}$$

where v is the relative velocity between the colliding particles, and $N_{\rm H}$ is the density of hydrogen atoms. The C_6 parameter (or any other parameter related to the damping width) is accurately known only for very few lines. The Unsold (1955, see also Gray 1976) approximation allows one to straightforwardly estimate the damping constants, but it has long been recognized that it underestimates the collisional broadening; and thus empirical enhancement factors are applied to C_6 in order to reproduce the observed line profiles.

The works by O'Mara (1976) and Anstee & O'Mara (1991) develop an alternative theory for the computation of cross sections σ of atomic transitions, thus providing a more accurate way to evaluate γ. Anstee & O'Mara (1995), Barklem & O'Mara (1997) and Barklem et al. (1998) published cross sections for a wide range of s-p and p-s, p-d and d-p, d-f, and f-d transitions, respectively. We refer to these cross-sections as ABO.

In order to use the more precise ABO theory in our calculations, we had to relate the ABO cross section σ to the classical interaction constant C_6 which is the input value to our spectrum synthesis code. The interaction constant can be expressed by:

$$C_6 = 6.46 \times 10^{-34} (R^2_{\rm hi} - R^2_{\rm lo}) \tag{A.2}$$

where $R^2_{\rm hi}$ and $R^2_{\rm lo}$ are the mean-square radii of the upper and lower states of the transition in atomic units. The cross section from the van der Waals theory is given by:

$$\sigma_{\rm vdW} = 63.65 (R^2_{\rm hi} - R^2_{\rm lo})^{2/5}. \tag{A.3}$$

From Eqs. (A.2) and (A.3), and replacing the classical cross-section $\sigma_{\rm vdW}$ by the cross-section given by ABO theory $\sigma_{\rm ABO}$, we obtain the relation:

$$C_6 = 6.46 \times 10^{-34} (\sigma_{\rm ABO}/63.65)^{5/2}. \tag{A.4}$$

Or in terms of γ_6:

$$\gamma_6/N_{\rm H} = 1.415 \times 10^{-14} v^{3/5} \sigma_{\rm ABO}. \tag{A.5}$$

The expression in Eq. (A.1) leads to a $\gamma \propto T^{2/5}$ relationship. However, according to the theory developed by ABO, which is based on the formalism by Brueckner (1971), γ has a dependence on the temperature that varies between $T^{0.3}$ and $T^{0.4}$. The ABO papers tabulate the velocity exponents α that take this non-universal dependence into account. Due to the different formalisms used by ABO theory and by the spectral synthesis code, the dependences of γ_6 on temperature are somewhat different. Nevertheless, the error introduced in the computed line profile is negligible (<5%) given other sources of errors like uncertainties in the atmospheric parameters, model atmospheres, and NLTE effects.

The $\sigma_{\rm ABO}$ values were obtained primarily from Barklem et al. (2000). Cross sections for lines not included in Barklem et al. (2000) were calculated through the code presented in Barklem et al. (1998). For this purpose, the energy levels and orbital angular momentum quantum numbers for each transition were obtained from the line list of Kurucz (1993), available at the web address `http://kurucz.harvard.edu/linelists`. The ionization limits of the transitions were approximated by the first ionization potential of the atom. Although this approximation is not strictly accurate, as pointed out in Barklem et al. (2000), the detailed inclusion of the ionization limits of each transition is beyond the scope of the present work.

A further step in critically evaluating the damping widths of the strongest lines is to take the model atmosphere adopted into account. This effect is illustrated for the Ca line 6162 Å in Fig. A.1. Cross sections for three lines of Ca I (Å = 6102, 6122, 6162) have been accurately calculated by Spielfiedel et al. (1991). The ratios $\gamma_{\rm ABO}/\gamma_{\rm Spielfiedel}$ for these lines are (0.8, 1.05, 0.96), which indicates good agreement. Figure A.1 shows the solar spectrum (solid line), a synthetic spectrum calculated using the solar model atmosphere by Holweger & Muller (1974, HM74, filled circles), and another synthetic spectrum calculated with ATLAS9 models (open circles). The C_6 employed is the one directly obtained from Eq. (A.4), using the same parameters as given in Anstee & O'Mara (1995), Table 3.

It can be seen that the line profile computed with the ATLAS9 model is stronger than when the HM74 model is used.

The use of an MARCS model atmosphere (Plez et al. 1992) results in a line profile that is very similar to the one obtained when the ATLAS9 model is employed.

The computed line profile depends on both the damping constant and the model atmosphere. Hence, even employing perfect damping parameters does not guarantee that correct profiles are computed, since the synthetic profile also depends on the adopted model atmosphere, as already pointed out by Cayrel et al. (1996) and Barbuy et al. (2003) and as is clearly shown in Fig. A1.

As a result, 5% of the lines for which the broadening values were calculated through ABO theory have wings that are too strong when compared with the observed spectrum of the Sun, when calculated with an ATLAS9 model. Therefore, the C_6 values for these lines were fitted manually to the solar spectrum. It was found that the average γ(ABO)/γ(best fit) for those lines is $\approx$1.4. Cayrel & Van't Veer (private communication) performed similar tests for the Mg I triplet lines, and found that γ(ABO)/γ(best fit) $\approx$1.5, which is in remarkable agreement with our own results.

The wings of the weaker lines are not critically affected by the use of different model atmospheres, as can be seen for the two weaker lines in Fig. A.1. This implies that for $\approx$95% of the lines, the broadening predicted by ABO theory fits the solar spectrum well when ATLAS9 models are employed.